MAPPING OF THE INTERSTITIAL IRON CONTENT IN MULTICRYSTALLINE SILICON BY MWPCD MEASUREMENTS

Kevin Lauer[1,2], Abdelazize Laades[1], Michael Blech[1] and Alexander Lawerenz[1]

[1]CiS Institut für Mikrosensorik GmbH, SolarZentrum Erfurt, Konrad-Zuse-Str. 14, 99099 Erfurt, Germany,
Phone: +49 - 361 - 663 12 22, Fax: +49 - 361 - 663 14 13, email: klauer@cismst.de
[2]Institut für Physik, TU-Ilmenau, Weimarer Str. 32, 98693 Ilmenau

ABSTRACT: In this paper the microwave-detected photoconductance decay (MWPCD) is evaluated in detail to allow a reliable determination of the interstitial iron content with high spatial resolution. The effect of the iron-boron-pair dissociation within a surface passivated solar grade silicon wafer on the MWPCD signal is demonstrated. An advanced evaluation method of the MWPCD signal is applied, revealing the minority carrier lifetime as a function of the excess carrier density. After the MWPCD signal is calibrated by a quasi-steady-state photoconductance (QSSPC) measurement, the interstitial iron content is calculated from the difference in the lifetime in both states of the iron-boron pairs. The interstitial iron content of a multicrystalline silicon wafer is mapped, showing a reduced content at the grain boundaries due to gettering. At the edge of a Czochralski silicon ingot an increasing interstitial iron content is found, which is caused by indiffusion from the gas ambient during ingot pulling.

Keywords: Photoconductivity, Lifetime, Impurities

1 INTRODUCTION

Iron is one of the most common and detrimental impurities in solar grade silicon. To a large extent iron is precipitated in the silicon and only a small fraction of is interstitially solved. The latter part induces states in the silicon band gap, which cause strong carrier recombination. Iron in solar grade silicon is often inhomogeneously distributed due to diffusion processes and agglomeration at other precipitates as well as crystalline defects. To understand these processes, it is of great interest to map the iron content. Fortunately, the content of the interstitial iron can be easily determined in boron doped silicon, exploiting the defect reaction with boron.

There are several techniques, which use the change in the minority carrier lifetime in both states of the iron-boron pairs in order to map the interstitial iron content. These are surface photo voltage (SPV) [1], infrared lifetime mapping (ILM) [2], photoluminescence (PL) [3] and microwave-detected photoconductance decay (MWPCD) [4] measurements. In this paper a reliable method to measure the interstitial iron content with the MWPCD system is developed. The differences compared to other methods are discussed and the applicability is demonstrated.

2 DETERMINATION OF THE INTERSTITIAL IRON CONTENT BY MWPCD MEASUREMENTS

2.1 Effect of the iron-boron-pair dissociation on the MWPCD signal

The MWPCD signal referred to as transient is measured using the commercial device WT-2000® from Semilab, which generates excess carriers by a laser pulse ($\lambda = 904$ nm) with a maximum intensity of 16.4 Wcm^{-2} and a spot size of about 1 mm^2. Measurements are done on boron doped and silicon nitride passivated [5] multicrystalline silicon or Czochralski silicon wafers, with a thickness below 200 µm. These wafers usually contain considerable amounts of interstitial iron, which forms in p-type silicon meta-stable pairs with the acceptor [6], e.g. boron. These iron-boron pairs are easily dissociated by illumination or heating of the sample. Association takes place if the wafer is stored in darkness at room temperature. Both states of the iron-boron pairs induce different states in the silicon band gap, which can be described by the Shockley-Read-Hall (SRH) theory [7]. Hence the dissociation of iron-boron pairs causes a change in the minority carrier lifetime. This is observed by a changing MWPCD signal during illumination of the sample as it is depicted in Fig. 1. The iron-boron pairs are dissociated using the excitation laser of the MWPCD system. In the iron-boron-pair state, only four transients are measured and averaged to avoid considerable pair breaking during the measurement. The measurements, which are taken in the intermediate and completely dissociated state, represent the average over 1024 transients to lower the noise of the signal.

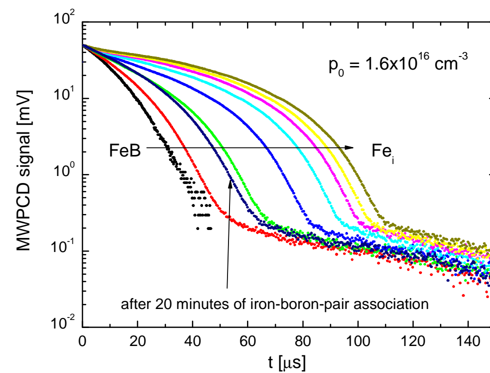

Fig. 1: MWPCD signal during the dissociation of the iron-boron pairs.

This defect reaction, which is often observed in solar silicon, might originate from other impurities in the solar silicon. Hence it has to be scrutinized if this defect reaction indeed originates from the iron-boron pairs. This can be done by investigating the association process. In boron doped silicon solely chromium is known beside iron to increase the lifetime in the mid to high injection region after illumination [8, 9]. Both contaminants differ in the time constants of the exponential lifetime decay during the association process. The association time

constant of chromium-boron pairs is found to be in the range of several hours [10] compared to the time constant for iron-boron pairs, which is in the range of minutes. Hence, if a pronounced change in the signal occurs several minutes after turning off the illumination (see Fig. 1), the defect reaction originates mainly from the iron-boron pairs.

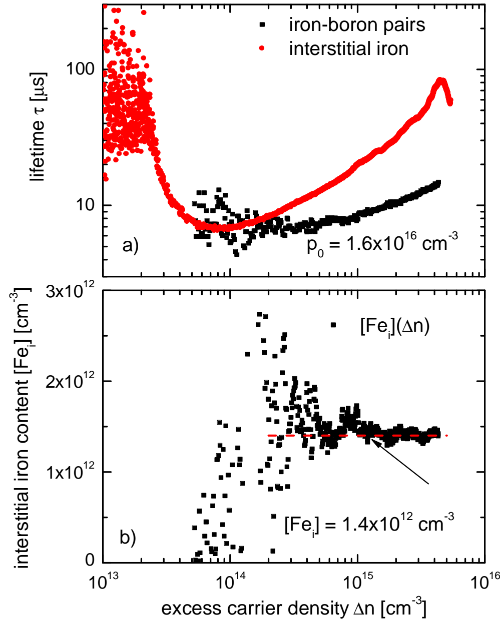

Fig. 2: a) Minority carrier lifetime plotted as a function of the excess carrier density in both states of the iron-boron pairs. b) Interstitial iron content is calculated from the data of part a) as a function of the excess carrier density.

2.2 Extraction of the minority carrier lifetime from the MWPCD signal

MWPCD measurements reveal a signal proportional to the excess carrier density [11]. To obtain absolute values of the excess carrier density the signal has to be calibrated. This point will be discussed in detail in section 3. Usually the MWPCD signal is fitted exponentially and the time constant of the decay is interpreted as the minority carrier lifetime. As can be seen in Fig. 1, this conventional evaluation method reveals only a bad approximation to the MWPCD signal and thus leads to a loss of information about the material. To overcome this problem an evaluation method was developed [12,13], which analyses the MWPCD signal at every time point as follows

$$\tau_b(t) \;=\; -\frac{1}{d(\ln \Delta n(t))/dt} \quad (1)$$

With this approach the minority carrier lifetime τ_b can be determined as a function of the excess carrier density Δn. But this evaluation method is only applicable, if thin ($w < 200\ \mu m$) and surface passivated wafers with minority carrier lifetimes in the range of about $1\ \mu s < \tau_b < 100\ \mu s$ are investigated [13]. Fig. 2a shows the MWPCD measurements of Fig. 1 in both states of the iron-boron pairs, which are evaluated using Eq. (1). The iron-boron-pair dissociation causes the typical change in the minority carrier lifetime as it can also be observed by quasi-steady-state photoconductance (QSSPC) measurements [14].

The anomalous increase in the lifetime at low excess carrier densities as observed in Fig. 2a is caused by the minority carrier trapping effect [15] and by the depletion region modulation effect (DRM) [16].

2.3 Calculation of the interstitial iron content

The difference in the minority carrier lifetime measured in both states of the iron-boron pairs can be used to determine the interstitial iron content. This method was first applied to surface photo voltage (SPV) measurements [17] and later extended to QSSPC measurements [18]. It relies on the complete knowledge of the SRH parameters in both states of the iron-boron pairs. If the lifetimes τ_{Fei} and τ_{FeB} are measured in the respective states, the interstitial iron content is given by [18]

$$[Fe_i] = C(\Delta n)\left(\frac{1}{\tau_{Fei}(\Delta n)} - \frac{1}{\tau_{FeB}(\Delta n)}\right) \quad (2)$$

The prefactor $C(\Delta n)$ is calculated using the SRH formalism with the parameters taken from Ref. [19] and Ref. [20] for the iron-boron pairs and interstitial iron, respectively. If the lifetimes are obtained for a large range of the excess carrier density, the interstitial iron content can be calculated as a function of the excess carrier density. Of course the interstitial iron content does not depend on the excess carrier density and hence should be constant, but this plot can be used to check the accuracy of the respective measurement method. The interstitial iron content calculated from the data displayed in Fig. 2a is plotted in Fig. 2b. An interstitial iron content of $[Fe_i] = 1.4 \cdot 10^{12}\ cm^{-3}$ is found, which is constant for the most part of the measurement revealing the evaluation approach of the MWPCD measurement to be accurate.

3 CALIBRATION OF THE MWPCD SIGNAL

The knowledge of the excess carrier density at which the minority carrier lifetime is extracted is crucial for the determination of the interstitial iron content. Hence, it will be discussed in more detail. There are three ways to calibrate the MWPCD signal. First the evaluated MWPCD signal can be compared to QSSPC measurements. Second the proportionality factor between MWPCD signal and excess carrier density can be calculated using a model [21]. And last the MWPCD signal can be approximated by a numerical simulation if the bulk lifetime in dependence of the excess carrier density is known [22]. The latter two methods are less applicable because the detailed setup of our commercial MWPCD setup is unknown and the bulk lifetime is the quantity, which has to be determined by the measurement. Hence the comparison of the MWPCD signal with QSSPC measurements will be used for calibration.

The QSSPC tool measures the photoconductance using an inductively coupled coil. This signal is calibrated to wafers with known resistivity. If the bulk lifetime of a wafer is a function of the excess carrier

density, the MWPCD signal can be calibrated by a QSSPC measurement. The evaluated MWPCD measurement is shifted horizontally until both lifetime curves coincide (see Fig. 3). This transformation determines the proportionality factor between MWPCD voltage and excess carrier density. Using the calibration by QSSPC measurements a problem arises due to the differing measurement spot sizes of MWPCD (~1 mm^2) and QSSPC (~1 cm^2). If the lifetime varies laterally, as is usually the case in multicrystalline silicon, the QSSPC and MWPCD measurements differ quite strongly. Hence in multicrystalline silicon a homogeneous region has to be used for calibration. To avoid this problem a mono crystalline Czochralski silicon wafer was taken for the measurements displayed in Fig. 3. This calibration routine has to be accomplished only once for one type of wafer, because it depends mainly on the doping of the silicon.

A detailed discussion of the differences between QSSPC and MWPCD signal is given in Ref. [13].

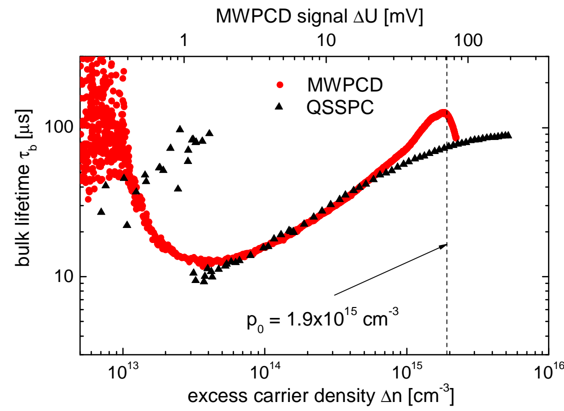

Fig. 3: The minority carrier lifetime of a Czochralski silicon wafer is measured by MWPCD and QSSPC. To calibrate the MWPCD signal the lifetime curve is shifted until it agrees with the QSSPC measurement.

4 MAPPING OF THE INTERSTITIAL IRON CONTENT

The approach described in section 2 can now be used to obtain two dimensional maps of the interstitial iron content using the MWPCD measurement system. There are several techniques to map the interstitial iron content. Two dimensional maps can be obtained using SPV [1]. This method is operating in low injection, hence the prefactor in Eq. (2) is well known. However, a measurement is time consuming, causing errors due to association of the iron-boron pairs during the mapping. The effect of the iron-boron-pair dissociation can also be visualized very fast by infrared lifetime mappings [2] and photoluminescence images [3]. In both cases the wafer is illuminated with a homogeneous light source. The measured signal of both methods is proportional to the excess carrier density, thus it has to be calibrated by a QSSPC measurement or by reference wafers. If the electronic quality of the investigated wafer is inhomogeneous, as is usually the case in multicrystalline silicon, the excess carrier profile will vary laterally under homogeneous illumination. This disturbs the calculation of the interstitial iron content from the images in both states of the iron-boron pairs, because the prefactor in Eq. (2) depends strongly on the excess carrier density. The last method to observe the effect of iron-boron-pair dissociation spatially resolved is the MWPCD measurement [4], using the conventional approach to evaluate the transient. This method also suffers from the unknown excess carrier density during the measurement. But also the linear fit to the transients as depicted in Fig. 1 leads to erroneous results.

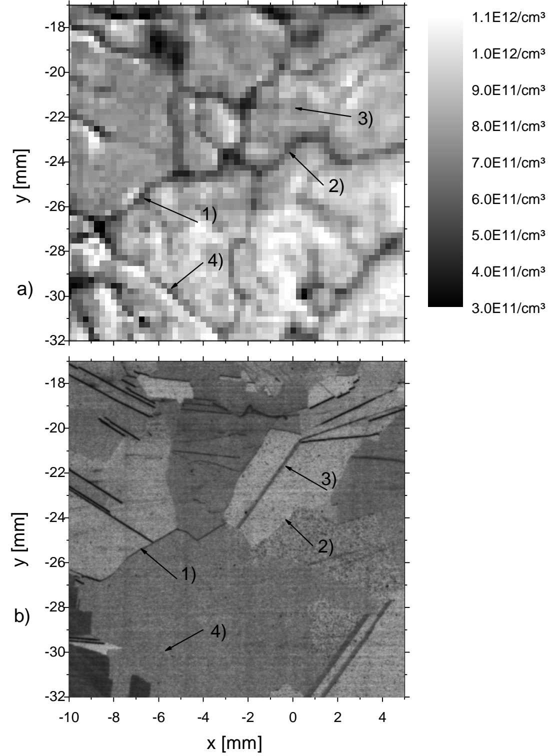

Fig. 4: The image of the interstitial iron content a) of a multicrystalline silicon wafer is compared to an optical scan image b) of the same wafer. The brightness of the scan image is inverted.

The problem of an unknown excess carrier density at each point can be avoided if the MWPCD signal is measured point by point and subsequently evaluated as described in section 2. Maps of the interstitial iron content, which are obtained by applying this method are displayed in Fig. 4a and Fig. 5a. In Fig. 4 a multicrystalline silicon wafer with a silicon nitride surface passivation is investigated. The image of the interstitial iron content is compared to a scan image of the wafer (see Fig. 4b). Clearly visible is a reduced interstitial iron content at the grain boundaries (see arrows 1 and 2 in Fig. 4a and b). The reduced iron content at the grain boundaries is caused by gettering. Unfortunately, not all grains are visible on the scan image (see arrow 4). Some grain boundaries do not show a decreased interstitial iron content as depicted by arrow 3 in Fig. 4b.

In Fig. 5 the border area of a Czochralski silicon ingot is investigated. In this region usually high iron contents are observed due to indiffusion of iron from the ambient gas during pulling of the ingot [23]. The image

of the interstitial iron content measured on a SiN_x passivated Czochralski silicon wafer is shown in Fig. 5a. Clearly visible is the decrease of the interstitial iron content from the border towards the center of the ingot. In Fig. 5b the average of the interstitial iron content in the y-direction is compared to the numerical solution of the iron diffusion equation [24]. It is assumed that the fraction of the interstitial iron content compared to the total iron content does not vary and is 0.01. Little is known in the literature about the temperature conditions during the ingot pulling, because such information is not disclosed by the companies. Hence a rough estimation of 7 h at 1000 °C is used to simulate the diffusion. The diffusion coefficient is taken from Ref. [20]. Nevertheless, a very good agreement between the measured and simulated iron content is found revealing the increased iron content at the edge of the ingot to be caused by solid state diffusion. The deviation of the measured iron content from the simulated one originates from the temperature profile within the ingot during the pulling process. The constant iron content, which is observed in the inner regions of the wafer, stems from iron contaminated silicon feedstock.

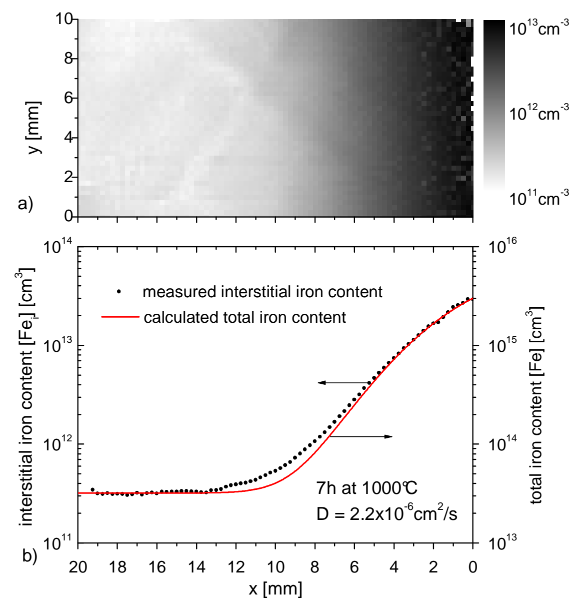

Fig. 5: a) Map of the interstitial iron content of a Czochralski silicon wafer. The border of the ingot is at x = 0. In part b) the average over y-direction is compared to a numerical solution of the iron in silicon diffusion equation.

5 CONCLUSION

The impact of the iron-boron-pair dissociation on the microwave-detected photoconductance decay (MWPCD) is analyzed and used to determine the interstitial iron content with high spatial resolution. Therefore, an advanced method to evaluate the MWPCD signal is applied. Two dimensional images of the interstitial iron content are taken from multicrystalline and Czochralski silicon wafers, which exemplify gettering of iron at the grain boundaries and indiffusion of iron from the gas ambient into the Czochralski ingot during the pulling process, respectively.

ACKNOWLEDGEMENT

The funding of this work by the State of Thuringia under project DEFIS (2006 WF 0100) is gratefully acknowledged.

REFERENCES

[1] G. Zoth and W. Bergholz, J. Appl. Phys. **67** (1990) 6764

[2] J. Henze, P. Pohl, C. Schmiga, M. Dhamrin, T. Saitoh, I. Yamaga, and J. Schmidt, in Proceedings of the 20th European Photovoltaic Solar Energy Conference (WIP-Munich, Germany, 2005), p. 769

[3] D. Macdonald, J. Tan, and T. Trupke, J. Appl. Phys. **103** (2008) 073710

[4] C. Swiatkowski, in Recombination Lifetime Measurements in Silicon, edited by D. C. Gupta, W. M. Hughes, and F. R. Bacher (ASTM, 1998), p. 80

[5] T. Lauinger, J. Schmidt, A. G. Aberle, and R. Hezel, Appl. Phys. Lett. **68** (1996) 1232

[6] K. Graff and H. Pieper, J. Electrochem. Soc **128** (1981) 669

[7] W. Shockley and W. Read, Phys. Rev. **87** (1952) 835

[8] K. Graff, Metal impurities in silicon-device fabrication (Springer, Berlin, 2000), 2nd ed.

[9] K. Kurita and T. Shingyouji, in Recombination Lifetime Measurements in Silicon, edited by D. C. Gupta, W. M. Hughes, and F. R. Bacher (ASTM, 1998), p. 59

[10] J. Schmidt, R. Krain, K. Bothe, G. Pensl, and S. Beljakowa, J. Appl. Phys. **102** (2007) 123701

[11] M. Kunst and G. Beck, J. Appl. Phys. **60** (1986) 3558

[12] K. Lauer, A. Laades, H. Übensee, A. Lawerenz and H. Metzner, Proc. 22nd Europ. PVSEC, Milano (2007) 1344

[13] K. Lauer, A. Laades, H. Übensee, H. Metzner, A. Lawerenz, J. Appl. Phys, submitted

[14] R. Sinton and A. Cuevas, Appl. Phys. Lett. **69** (1996) 2510

[15] D. Macdonald and A. Cuevas, Appl. Phys. Lett. **74** (1999) 1710

[16] D. H. Neuhaus, P. J. Cousins, and A. G. Aberle, in Proceedings of the 3rd World Conference on Photovoltaic Energy Conversion (IEEE, New York, 2003)

[17] G. Zoth and W. Bergholz, J. Appl. Phys. **67** (1990) 6764

[18] D. Macdonald, L. Geerligs and A. Azzizi, J. Appl. Phys. **95** (2004) 1021

[19] D. Macdonald, A. Cuevas, and J. Wong-Leung, J. Appl. Phys. **89** (2001) 7932

[20] A. Istratov, H. Hieslmair, E. Weber, Appl. Phys. A **69** (1999) 13

[21] M. Schoefthaler and R. Brendel, J. Appl. Phys. **77** (1995) 3162

[22] K. Lauer, A. Laades, A. Lawerenz, Mat. Sci. Eng. B, submitted

[23] K. Harada, H. Tanaka, J. Matsubara, Y. Shimanuki, H. Furuya, J. Cryst. Gr. **154** (1995) 47-53

[24] I. Wolfram Research, Mathematica Edition: Version 6 (Wolfram Research, Inc., 2007)